Available online at www.sciencedirect.com
ScienceDirect
Journal of the European Ceramic Society 28 (2008) 27–34
www.elsevier.com/locate/jeurceramsoc

Reactivity and stability of rare earth oxide–Li_2CO_3 mixtures

Mitsuru Yamauchi, Yoshiteru Itagaki, Hiromichi Aono*, Yoshihiko Sadaoka

Department of Materials Science and Biotechnology, Graduate School of Science and Engineering, Ehime University, Matsuyama, Ehime 790-8577, Japan

Received 19 April 2007; accepted 9 June 2007
Available online 13 August 2007

Abstract

The thermal stability of a mixture of Li_2CO_3 and rare earth oxide (R_2O_3) was examined under a dry condition. The heat-treatment of the mixture in CO_2 ambience resulted in the formation of rare earth carbonates for R = La, Pr, Nd, Sm, Eu, and Gd except for Ho–Lu and Y. Lithiation of their rare earth dioxymonocarbonate, i.e., $R_2O_{2+2x}(CO_3)_{1-x}Li_{2x}$ was confirmed for R = La, Pr, Nd, and Sm when the mixture was heated at 900 °C. The lithiation degree, x, was increased with an increase in the heat-treatment temperature in CO_2 and was lower than 0.3. The stability of lithium rare earth dioxymonocarbonate decreased with the atomic number of the rare earth. The high reactivity of the light rare earth oxides with Li_2CO_3 would be attributed to that the large R^{3+}–O^{2-} distance for CN = 5 and 6 with an increase in the ionic $[R^{3+}]/[O^{2-}]$ ratio for the rare earth oxides and is very similar with that of the rare earth dioxymonocarbonates.

Keywords: Powders-solid state reaction; Powders-gas phase reaction; X-ray methods; Sensors; Rare earth dioxymonocarbonate; Li_2CO_3

1. Introduction

The increasing need for reliable and continuous monitoring of CO_2 levels in the atmosphere has promoted the development of potentiometric sensors using a cation conducting solid electrolyte and an auxiliary phase on the measuring electrode.[1–5] A potentiometric CO_2 sensor with a Li_2CO_3 layer as an auxiliary electrode shows satisfactory performances with a fast response, appreciable sensitivity and gas selectivity. However, the sensors show a lack of reproducibility and long-term stability.[6–11] To improve the long-term stability, a new auxiliary electrode material based on Li_2CO_3 and Nd_2O_3 was developed.[12,13] We also confirmed similar additive effects on the sensing performance for several rare earth oxides. When only Li_2CO_3 was used as an auxiliary electrode in a lower level of CO_2, the concentration of Li_2O in the layer increased, and the formed oxide reacted with a solid electrolyte such as a NASICON. For a mixture of Li_2CO_3 and rare earth oxide, the formation of rare earth carbonate and oxycarbonate is expected. The rare earth carbonates and their decomposition and synthesis had been the subject of many investigations. The thermal decomposition of anhydrous rare earth carbonate to oxide occurs *via* intermediate oxycarbonate phases. The stoichiometric rare earth oxycarbonates are monoxydicarbonate, $R_2O(CO_3)_2$, and dioxymonocarbonate, $R_2O_2CO_3$. Attfield and Ferey reported that the lithium-containing lanthanum dioxycarbonate type phase ($La_2O_{2+2x}(CO_3)_{1-x}Li_{2x}$, $x = 0.26$) was formed when a mixture of La_2O_3 and Li_2CO_3 was heated at 550 °C in air.[14] In our previous studies, we investigated the formation of a lithiated rare earth dioxycarbonate, $Nd_2O_{2+2x}(CO_3)_{1-x}Li_{2x}$ using a mixture of Nd_2O_3 and Li_2CO_3 in CO_2.[15] In this case, pure Nd_2O_3 did not react with CO_2 gas to form the $Nd_2O_2CO_3$ at all. However, the $La_2O_2CO_3$ was easily formed by the reaction of a pure La_2O_3 with CO_2.[16]

In this work, the reactivity of Li_2CO_3 with a variety of rare earth oxides and the heat treatment of the mixture in CO_2 were examined to develop new auxiliary electrode materials for a potentiometric CO_2 gas sensor. Especially, the thermal stability of the mixtures and thermal products were examined.

2. Experimental

Commercially available rare earth oxalates of $La_2(C_2O_4)_3 \cdot 9H_2O$ and $Ln_2(C_2O_4)_3 \cdot 10H_2O$ (Ln = Nd, Gd, Dy, and Ho) (99.9%), rare earth oxides (99.9%) and Li_2CO_3 (99.9%) were

* Corresponding author.
E-mail address: haono@eng.ehime-u.ac.jp (H. Aono).

0955-2219/$ – see front matter © 2007 Elsevier Ltd. All rights reserved.
doi:10.1016/j.jeurceramsoc.2007.06.013

used as starting materials. The rare earth oxides powders were pre-heated at 400 °C in air before the mixing. Mixtures of an oxide and Li_2CO_3 at a 1:1 molar ratio were pulverized and mixed under dry condition by ball milling in a Nylon pot and with Y-stabilized zirconia balls. Thermal studies were carried out with thermogravimetric analysis (TGA) and differential thermal analysis (DTA) under synthesized air (syn-air, <0.5 ppm CO_2) and 100% CO_2 for the mixtures at a heating and cooling rate of 5 °C/min. The crystal structure and the components of the mixtures were examined by the powder XRD method (Cu Kα).

3. Results

3.1. Formation of carbonates

For the mixtures of R_2O_3 and Li_2CO_3, the formations of some compounds such as $R_2(CO_3)_3$, $R_2O(CO_3)_2$, $R_2O_2CO_3$, and $LiR(CO_3)_2$ are expected by the heat treatment in CO_2. The rare earth ions should react in ground water with a 100–200 ppm carbonate ion concentration to form $[RCO_3]^+$ and $[R(CO_3)_2]^-$ complexes, although $R_2(CO_3)_3$ is the most stable solid carbonate phase under these conditions. The water molecules of rare earth carbonate hydrate are released in a single stage somewhere between 150 and 300 °C. Furthermore, the thermal decomposition of anhydrous rare earth carbonate to oxide occurs via intermediate oxycarbonate phases. The stoichiometric oxycarbonates are monooxydicarbonate, $R_2O(CO_3)_2$, and dioxymonocarbonate, $R_2O_2CO_3$. The decomposition of anhydrous rare earth carbonates begins above 350 °C. In air and CO_2 atmosphere, the formation of $R_2O(CO_3)_2$ has been reported for the lighter lanthanides.[17,18] The stability of the oxycarbonate phase in air decreased with the increasing atomic number of the rare earth.[19] $Nd_2O_2CO_3$, for example, is stable in air to 750 °C and $La_2O_2CO_3$ is stable in CO to nearly 1000 °C.[20] Solid state rare earth carbonates can be prepared by the following two precipitation methods: (1) by adding alkali or ammonium carbonate or hydrogen carbonate to a solution of the metal salt and (2) by passing carbon dioxide through an aqueous suspension of the metal hydroxide. The ternary carbonates $LiR(CO_3)_2$ with R = La to Lu and Y were synthesized from mixtures of lithium carbonate and $R_2(C_2O_4)_3{\cdot}xH_2O$ under 2000 atom CO_2 and 500 °C.[21]

For rare earth oxides heated in CO_2, the following reactions are expected:

$$R_2O_3 + 3CO_2 \rightarrow R_2(CO_3)_3 \quad (1)$$

$$R_2O_3 + 2CO_2 \rightarrow R_2O(CO_3)_2 \quad (2)$$

$$R_2O_3 + CO_2 \rightarrow R_2O_2CO_3 \quad (3)$$

$$R_2O_3 + xCO_2 \rightarrow R_2O_{2+x}(CO_3)_{1-x} \text{ or } R_2O_3{\cdot}xCO_2 \quad (4)$$

In the case of hydrous rare earth oxalates decomposed by heat treatments in air, the decomposition steps are described as

$$R_2(C_2O_4)_3{\cdot}nH_2O \rightarrow R_2(C_2O_4)_3 \rightarrow R_2(C_2O_4)(CO_3)_2 \rightarrow R_2(CO_3)_3 \rightarrow R_2O(CO_3)_2 \rightarrow R_2O_2CO_3 \rightarrow R_2O_3 \quad (5)$$

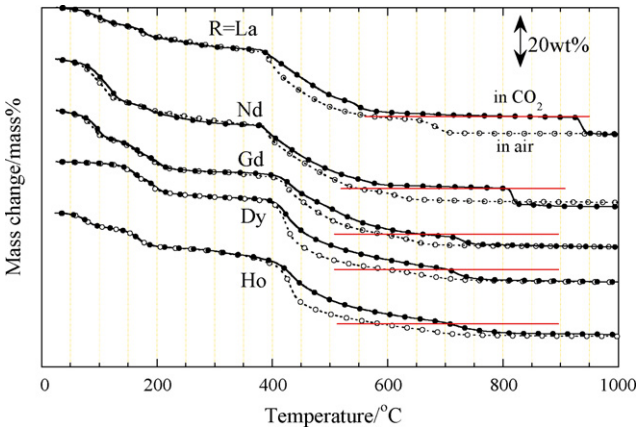

Fig. 1. TGA results for rare earth oxalates $R_2O_2CO_3{\cdot}nH_2O$ (R = La, Nd, Gd, Dy, and Ho) in air (◯) and in CO_2 (●).

Fig. 1 shows the TGA results in syn-air and CO_2 for some oxalates. In the thermal decomposition of the hydrous oxalates at a constant heating rate, the anhydrous carbonate, $R_2(C_2O_4)_3$ was formed at around 380 °C and then the weight decreased in air and CO_2. For La-oxalate, the weight decreased in two steps and decomposed to La_2O_3 at 690 and 940 °C in air and CO_2, respectively. The weight estimations suggested the formation of $R_2O_2CO_3$ for R = La–Gd, and its decomposition temperature to R_2O_3 is 940, 815 and 730 °C for La, Nd and Gd in CO_2, respectively. The formation of the $R_2O_2CO_3$ single phase for R = La and Nd by the heat treatment of the rare earth oxalates in CO_2 was confirmed using XRD. The results and the estimated lattice parameters were fairly agreed with the published information in ICSD files (No. 202988: $La_2O_2CO_3$, hexagonal, *P*63/*mmc*, No. 6297: $Nd_2O_2CO_3$, hexagonal, *P*63/*mmc*). In air, the formed $R_2O_2CO_3$ decomposed to R_2O_3 at 700 and 630 °C for La and Nd, respectively. In addition, any plateau region could not be observed for the heavier rare earth oxalates of R = Gd, Dy, and Ho. It was concluded that the stability of $R_2O_2CO_3$ decreased in air and CO_2 ambient with the atomic number of the rare earth (R = La, Nd, Gd, Dy and Ho).

3.2. Heat-treated products of the mixture

To clarify the effects of the ambient on the thermal stability of the 1:1 mixtures of lithium carbonate and rare earth oxides, thermal studies were carried out under syn-air and CO_2 ambient at a constant heating rate of 5 °C/min. The TGA results of the mixtures in syn-air and CO_2 are shown in Figs. 2 and 3 for the light (La–Gd) and heavy (Dy–Lu) rare earths with Y, respectively. For the La_2O_3 system in CO_2, the weight increased gradually to 700 °C with temperature. A further heating resulted in a gradual decrease and a following a steep decrease at 960 °C. It should be noted that the weight observed at 980 °C is comparable to that of the starting mixture. In the heating process, the melting of Li_2CO_3 was detected at 716 °C by DTA, which is comparable to that of only Li_2CO_3. This observed coincidence suggests that Li_2CO_3 is stable in CO_2 even in the melted phase. An increase and a following decrease in the weight was confirmed also for the mixture for R = Pr, Nd, Sm, Eu and Gd. For CeO_2 and R_2O_3

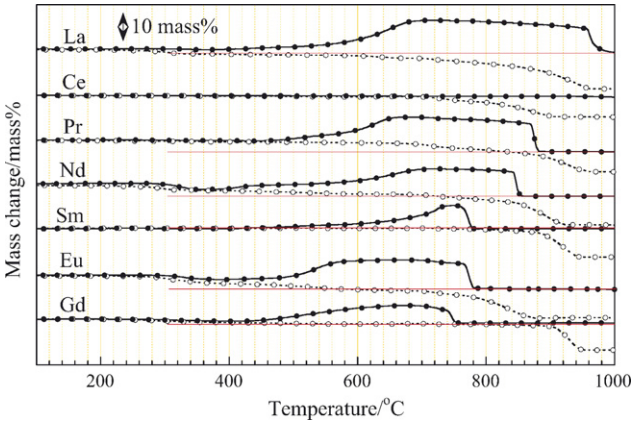

Fig. 2. TGA results of mixture (1:1 mol ratio) of R_2O_3 (La, Nd, Sm, Eu, and Gd), CeO_2, Pr_6O_{11} and Li_2CO_3 in syn-air (broken lines) and 100% CO_2 (solid lines). Critical points were determined by DTA.

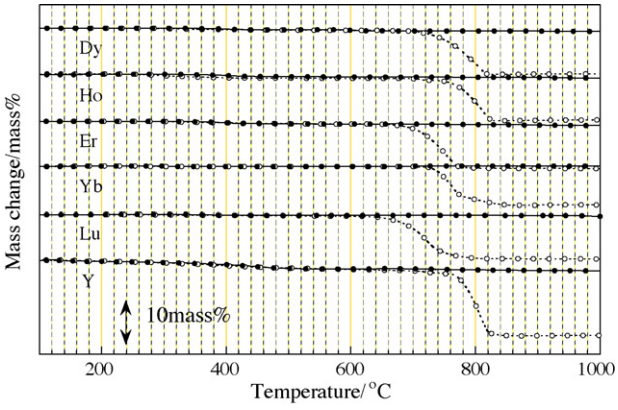

Fig. 3. TGA results of mixture (1:1 mol ratio) of R_2O_3 (Dy, Ho, Er, Yb, Lu, and Y) and Li_2CO_3 in syn-air (broken lines) and 100% CO_2 (solid lines). Critical points were determined by DTA.

(R = Dy–Lu and Y) systems; the weight remained a constant to 1000 °C in CO_2 in the heating process. On the other hand, the weight in syn-air decreased with the Li_2CO_3 decomposition to Li_2O at elevated temperature for all the mixed systems examined.

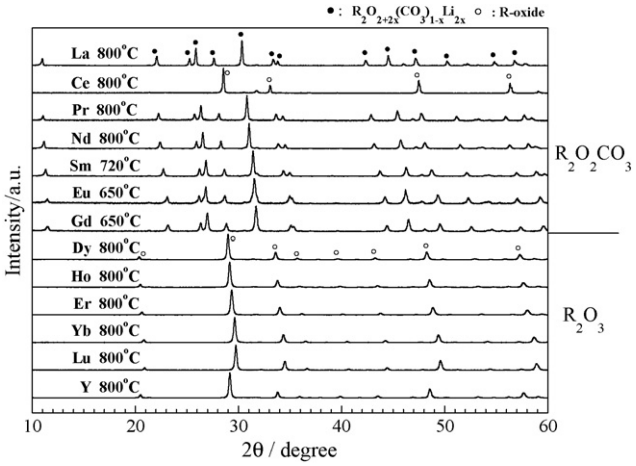

Fig. 4. XRD results at RT of the 1:1 mixture of Li_2CO_3 and rare earth oxides heat treated at various temperatures for 2 h in CO_2. RE and treatment temperature in °C are indicated in the figure.

The mixtures heat-treated in the range of 300 and 900 °C in syn-air and CO_2 ambient for 2 h were examined by XRD at room temperature. The XRD patterns of the mixture heat treated in CO_2 are shown in Fig. 4. The heated temperature for the examined samples was 800 °C except for Sm at 720 °C and Eu, Gd at 650 °C, because the maximum weight was obtained in TGA results (Fig. 2). The formations of the rare earth oxycarbonates were confirmed except for Ce and Dy–Lu, Y. The XRD patterns of the mixtures for R = La, Pr–Gd were very similar, and the peak positions showed a regular shift to a higher angle from La to Gd. These materials would be the lithiated rare earth dioxycarbonates, $R_2O_{2+2x}(CO_3)_{1-x}Li_{2x}$.[16] The metal oxide, R_2O_3, was only detected for R = Dy–Lu and Y, while the Li_2CO_3 phase was difficult to detect because the intensity of Li_2CO_3 was very weak. The peaks for the mixture of Y_2O_3 were situated between those for Ho_2O_3 and Er_2O_3 because of its ionic radius. The heat-treated products in CO_2 assigned from the XRD patterns are summarized in Table 1. At this stage, the rare earth dioxymonocarbonate and the Li-inserted rare earth dioxymonocarbonate are expressed as ROC, because the XRD patterns of both compounds are very similar. For the mixture of

Table 1
Phases of the mixtures (1:1 mol ratio) heated from 300 to 1000 °C in CO_2 for 2 h

R-oxide	500 °C	600 °C	700 °C	800 °C	900 °C	1000 °C
La_2O_3	O + LaOC	LaOC	LaOC	LaOC	LaOC	O + LaOC
CeO_2	O	O	O	O	O	O
Pr_6O_{11}	PrOC	PrOC	PrOC	PrOC	O + PrOC	O + PrOC
Nd_2O_3	O + NdOC	NdOC	NdOC	NdOC	O + NdOC	O
Sm_2O_3	O	O + SmOC	O + SmOC	O + SmOC	O	O
Eu_2O_3	EuOC	EuOC	EuOC	O	O	O
Gd_2O_3	O + GdOC	O + GdOC	O + GdOC	O	O	O
Dy_2O_3	O	O	O	O	O	O
Ho_2O_3	O	O	O	O	O	O
Er_2O_3	O	O	O	O	O	O
Yb_2O_3	O	O	O	O	O	O
Lu_2O_3	O	O	O	O	O	O
Y_2O_3	O	O	O	O	O	O

Remarks—O: rare earth oxide; ROC: rare earth dioxycarbonate.

Table 2
Phases of the mixtures (1:1 mol ratio) heated from 300 to 1000 °C in syn-air for 2 h

R-oxide	500 °C	600 °C	700 °C	800 °C	900 °C	1000 °C
La_2O_3	O	O	O	O	O + $LiLaO_2$	O
CeO_2	O	O	O	O	O	O + Li_8CeO_6
Pr_6O_{11}	O	O	O	O + $Li_{26}Pr_{36}O_{73}$	O + $Li_{26}Pr_{36}O_{73}$	O + $Li_{26}Pr_{36}O_{73}$
Nd_2O_3	O	O	O	O	O + $LiNdO_2$	O + $LiNdO_2$
Sm_2O_3	O	O	O	O	O + $LiSmO_2$ + D	O + $LiSmO_2$ + D
Eu_2O_3	O	O	O	O	O + $LiEuO_2$ + D	O + $LiEuO_2$ + D
Gd_2O_3	O	O	O	O	O + $LiGdO_2$ + D	O + $LiGdO_2$ + D
Dy_2O_3	O	O	O	O + $LiDyO_2$	O + $LiDyO_2$	O + $LiDyO_2$
Ho_2O_3	O	O	O	O	O + $LiHoO_2$	O + $LiHoO_2$
Er_2O_3	O	O	O + $LiErO_2$	O + $LiErO_2$	O + $LiErO_2$	O + $LiErO_2$
Yb_2O_3	O	O	O	O	O + $LiYbO_2$ + ?	O + $LiYbO_2$ + ?
Lu_2O_3	O	O + $LiLuO_2$	O + $LiLuO_2$	O + $LiLuO_2$	O + $LiLuO_2$	O + $LiLuO_2$
Y_2O_3	O	O	O	O	O + $LiYO_2$	O + $LiYO_2$

Remarks—O: rare earth oxide; $LiRO_2$: lithium rare earth oxide; D: disordered phase; ?: unknown.

Li_2CO_3 and light rare earth oxide except for CeO_2, ROC was formed. For the mixture of heavy rare earth and Y oxides, the XRD pattern was hardly changed by the heat treatment in CO_2. Furthermore, the products of the heat treatment in syn-air were examined by XRD, and the results are summarized in Table 2. The formation of $LiRO_2$ was confirmed, and the forming temperature has a tendency to decrease with an increase in the atomic number of rare earth except for CeO_2. For PrO_{2-x}, the product at 800 °C could be assigned to be $Li_{26}Pr_{36}O_{73}$.

The following reactions are expected:

$$R_2O_3 + Li_2CO_3 + 3CO_2 \rightarrow 2LiR(CO_3)_2 \quad (6)$$

$$R_2O_3 + Li_2CO_3 + CO_2 \rightarrow 2LiROCO_3 \quad (7)$$

$$R_2O_3 + Li_2CO_3 + CO_2 \rightarrow R_2O_2CO_3 + Li_2CO_3 \quad (8)$$

$$R_2O_3 + Li_2CO_3 \rightarrow R_2O_{2+2x}(CO_3)_{1-x}Li_{2x} + (1-x)Li_2CO_3 \quad (9)$$

in CO_2 and

$$R_2O_3 + Li_2CO_3 \rightarrow 2LiRO_2 + CO_2 \quad (10)$$

in syn-air.

The mixtures for R = La and Nd systems were heat treated at several temperatures in CO_2 to clarify the crystal structure changes with the treatments. The lattice parameters of ROC obtained using the heat treatment of the mixture at 600 °C were comparable to those using the heat treatment of the corresponding oxalates (Fig. 1) for $La_2O_2CO_3$ and $Nd_2O_2CO_3$. The *c*-lattice parameter increased and the *a*-lattice parameters decreased with an increase in the heat-treatment temperature as shown in Fig. 5. The increase in the lattice parameters with an increase in the heat-treatment temperature was due to the lithiation of rare earth oxycarbonate, i.e., the formation of the $R_2O_{2+2x}(CO_3)_{1-x}Li_{2x}$ phase.

From the expected reactions (8) and (9), the lithiation of rare earth oxycarbonates resulted in a decrease in the weight of the mixture. It is very difficult to determine the lithiation degree of the carbonate indirectly. The weight changes in the heating process in syn-air were examined for the heat-treated mixtures at 700, 800, and 900 °C in CO_2. The typical TGA results in syn-air are shown in Fig. 6. For example, the weight remained a constant to 620 °C and then decreased in two steps for R = Nd. During the same heating rate in syn-air, thermally programmed XRD measurement was applied (Fig. 7). The XRD signals due to $R_2O_{2+2x}(CO_3)_{1-x}Li_{2x}$ were detected to 600 °C, and its decomposition with the formation of Nd_2O_3 and Li_2CO_3 were confirmed at a higher temperature. The weight at 950 °C was comparable to that of the mixture of Li_2O and Nd_2O_3. It is assumed for convenience that the mixture heat treated in CO_2 is composed of a mixture of $R_2O_{2+2x}(CO_3)_{1-x}Li_{2x}$ and $(1-x)Li_2CO_3$, so that the weight loss observed in a lower temperature region is due to the decomposition of $R_2O_{2+2x}(CO_3)_{1-x}Li_{2x}$ to R_2O_3 and xLi_2O and the final plateau region is corresponds to the 1:1 mixture of R_2O_3 and Li_2O. The lithiation degree, *x*, could be estimated from the TGA results in syn-air as shown in Fig. 6. Before the estimation of the lithiation degree, it should be noted that the increment in the weight is strongly influenced by the maximum treatment temperature. The lithiation degree, *x*, was estimated to be 0.22, 0.13 and 0.06 for the mixtures heat treated at 900, 800, and

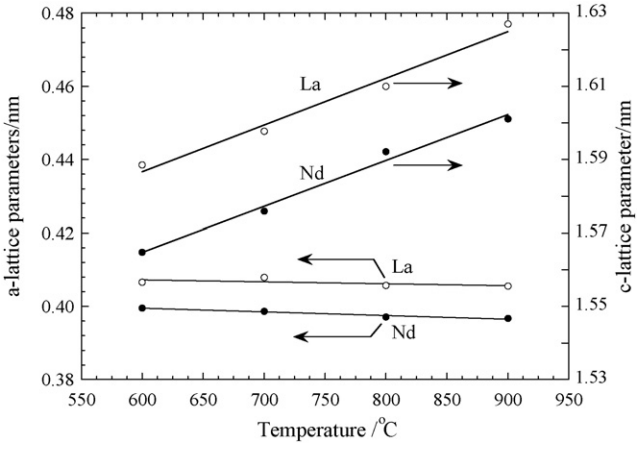

Fig. 5. Estimated lattice parameters from the newly observed XRD patterns at RT of the 1:1 mixture of Li_2CO_3 and R_2O_3 pre-heat treated in CO_2.

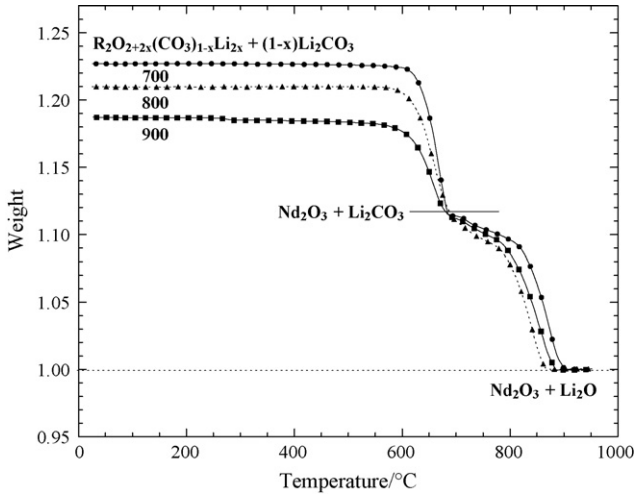

Fig. 6. TG results in syn-air of the 1:1 mixtures of Li_2CO_3 and Nd_2O_3 pre-heated in 100% CO_2 gas for 2 h. The heat treatment temperature in °C is denoted in the figure.

700 °C, respectively. The mixture of Li_2CO_3 and Nd_2O_3 was heat treated at several temperatures in CO_2 and then cooled to room temperature also in CO_2. TGA results in CO_2 for the pre-heat treated mixture of Nd_2O_3 and Li_2CO_3 are shown in Fig. 8. The heat treatment at 900 °C in CO_2 induced the decomposition of $R_2O_{2+2x}(CO_3)_{1-x}Li_{2x}$, and the reformation is progressed during the cooling process. The degree of the weight loss during the heating process decreased with an increase in the pre-heat treatment temperature from 700 to 900 °C. The lithiation degree increased with an increase in the treatment temperature. As shown in Fig. 2, the heating in CO_2 resulted in an increase in the weight and then decreased to the weight corresponding to the mixture of R_2O_3 and Li_2CO_3. Especially for R = Pr–Gd, the observed weight at a higher temperature around 900 °C corresponded to the mixture of R_2O_3 and Li_2CO_3. For the mixture heated at 900 °C, an increase in the weight was observed during the cooling process in CO_2 (Fig. 8). As not shown in the figure, the increase in the weight in the cooling process was also observed for R = La, Pr, Nd and Sm, but not for R = Eu

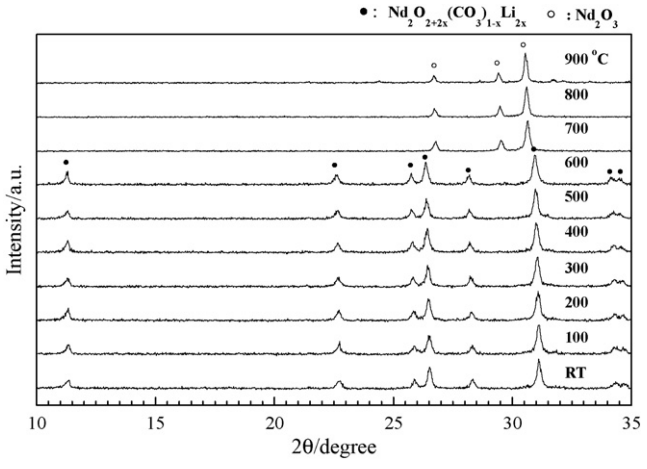

Fig. 7. Thermally programmed XRD pattern of the 1:1 mixture of Li_2CO_3 and Nd_2O_3 in CO_2. The measured temperature in °C is indicated in the figure.

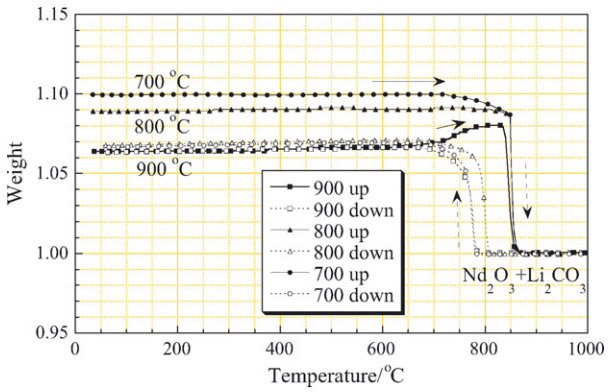

Fig. 8. TGA result of $Nd_2O_2CO_3$ (the mixture of 1:1 Nd_2O_3 and Li_2CO_3 heated at 700, 800, and 900 °C in 100% CO_2 for 2 h) in 100% CO_2.

and Gd. It seems that the reaction rate of the formation of $R_2O_{2+2x}(CO_3)_{1-x}Li_{2x}$ for R = Eu and Gd is very slow. For the mixture heated at 900 °C in CO_2, the lithiation degree was estimated to be 0.23, 0.14, 0.22 and 0.21 for R = La, Pr, Nd and Sm systems, respectively.

The lattice parameters of the heat-treated products were estimated by assuming hexagonal, *P*63/*mmc*. The correlation between the lithiation degree, *x*, and lattice parameters is shown in Fig. 9. It was concluded that the lithiation degree is monotonically increased with an increase in the *c*-lattice parameter. It should be noticed that the lithiation degree is clearly lower than 0.3. Attfield and Ferey reported that the lithium-containing lanthanum dioxycarbonate type phase ($La_2O_{2+2x}(CO_3)_{1-x}Li_{2x}$, $x = 0.26$) was formed when a mixture of La_2O_3 and Li_2CO_3 was heated at 550 °C in air for 11 days.[14]

For the mixture of heavy rare earth (and Y) oxides, the weight loss in CO_2 could not be observed to 1000 °C (Fig. 3), while the loss due to the decomposition of Li_2CO_3 to Li_2O was observed at around 700 °C in syn-air. The decomposition induced the formation of $LiRO_2$ as shown in Table 2. By the XRD technique, the phase changes and new products were not detected for the mix-

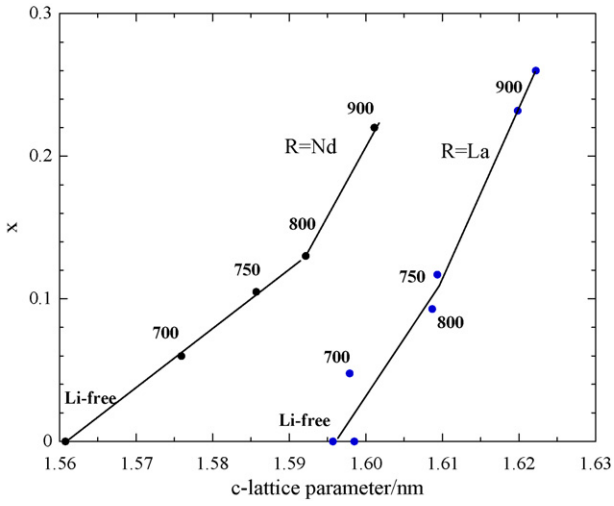

Fig. 9. Correlation between lithiation degree *y* and *c*-lattice parameter of $R_2O_{2+2y}(CO_3)_{1-y}Li_{2y}$. The Li-free carbonate was prepared from the corresponding oxalate.

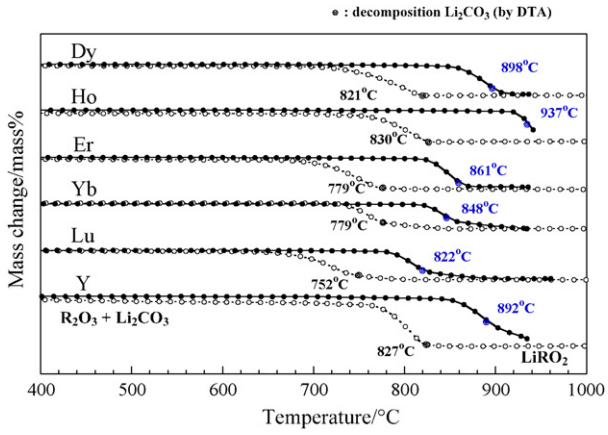

Fig. 10. TG results in air of the 1:1 mixture of R_2O_3 and Li_2CO_3 with and without pre-heat treatment in CO_2 to 950 °C.

ture of Li_2CO_3 and heavy rare earth (and Y) oxides in CO_2. The heat treatment of the mixture at 950 °C in CO_2 induced a change in the thermal stability of the mixture, especially, the Li_2CO_3 phase. In Fig. 10, TG results in syn-air are shown for the mixture before and after the heat treatment. As can be seen, the starting temperature of the weight loss is clearly shifted to a higher temperature. For the mixture both before and after the heat treatment, the melting point of Li_2CO_3 is observed at around 715 °C and is hardly influenced by the treatment and the rare earth element. It seems that the heat treatment in CO_2 induced the formation of carbonates on the surface of the rare earth oxides.

4. Discussion

For the mixtures of Li_2CO_3 and the heavy rare earth oxide (R = Dy–Lu), the weight in CO_2 remained constant to 1000 °C (Fig. 3). For R = Eu and Gd systems, the weight of the heat-treated mixture corresponded to the mixture of $R_2O_2CO_3$ and Li_2CO_3. For R = La, Pr, Nd, and Sm, the formation of the mixture of lithiated $R_2O_{2+2x}(CO_3)_{1-x}Li_{2x}$ and $(1-x)Li_2CO_3$ was confirmed by the TGA results as explained.

In general, the surface charge density of the cation decreases with an increase in the ionic size of the cation. It is expected the lattice energy increases with a decrease in the ionic size. The configuration of anions around the cation is mainly determined by the ratio of the cation. The coordination number (CN) of the cation is related to the counter anion and is a function of the ratio of cation and anion radii. Based on the geometrical analysis for ball closed packing stacking, the minimum radius ratio of cation and anion radii for 6-fold, 8-fold and 12-fold coordination is given as 0.414, 0.732 and 1.000, respectively. A close packed structure becomes unstable, and the occupancy (packing stacking fraction) decrease, with an increase in the ratio of cation/anion radii. After all, the coordination number increases with the ionic radius. Correlation between the radius ratio, $r(R^{3+})/rO^{2-}$ and the ionic radius of R^{3+} (atomic number of R) for sixfold and eightfold coordination is shown in Fig. 11. For larger rare earth metals (R = La through Gd), the radius ratio for eightfold coordination is higher than 0.73. The ratio (0.73) for Tb is in agreement with the minimum radius ratio for eightfold

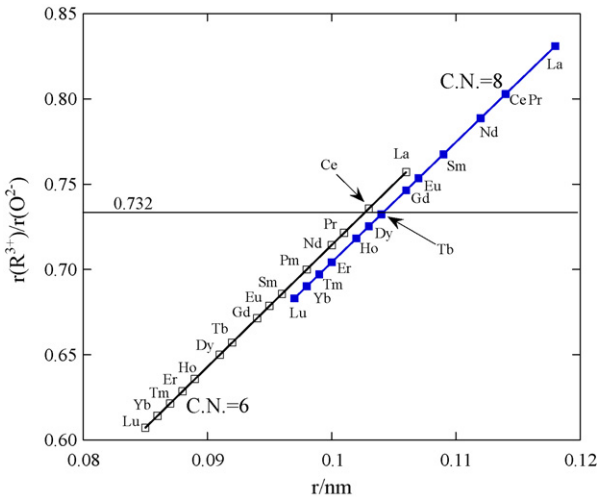

Fig. 11. Correlation between ionic radius of R^{3+} and radius ratio. Coordination number, CN, of R^{3+} is shown in the figure. $r(R^{3+})$ from Ref. [22]. O^{2-}(CN 6) = 0.140 nm, O^{2-} (CN 8) = 0.142 nm.

coordination. To remain an octahedral site (CN = 6) for R with oxygen, the ratio of cation and anion radii is confined within the range of 0.732 and 0.414. The radius ratio of Ce^{3+} for the sixfold coordination is 0.735, and rare earth ions coordinated with six oxygen ions except for $Ce^{3+}$and La^{3+}, are stable.

The crystal structure of the rare earth oxides used was determined by XRD. For La_2O_3 and Nd_2O_3, the crystal structure is well expressed with $P\bar{3}m1$ having the square $(R_2O_2^{2+})_n$ layers. The rare earth ion is surrounded by four oxygen ions in the 2d site and three oxygen ions in the 1a site situated in the (0 0 2) plane. Especially, the oxygen ions at the 1a site are only weakly interact with R ions. It seems that the formation of the oxycarbonate progresses without any distinct deformations of the square $(R_2O_2^{2+})_n$ layers for La_2O_3 and Nd_2O_3. The distance between the rear earth ion and coordinated oxygen are summarized in Figs. 12 and 13. The characteristics of R_2O_3 are referenced from the published data in ICSD files. The distance between R and the coordinated oxygen for CN = 4 is increased monotonically with an increase in the ionic radii of the R-ion. Although the distance between R and the oxygen for CN = 5

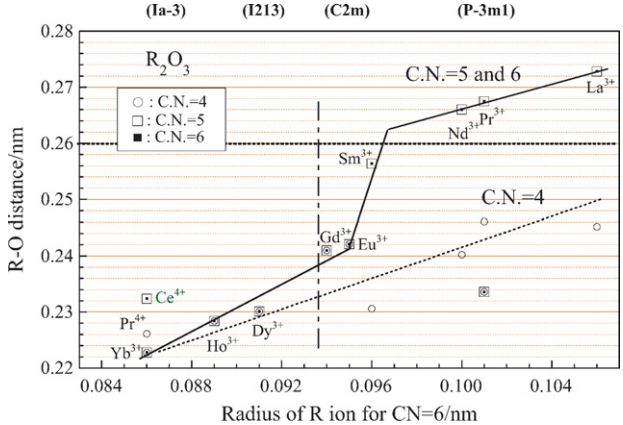

Fig. 12. Distance between the rare earth ion and coordinated oxygens of the rare earth oxides for CN = 4 and CN = 5 and 6.

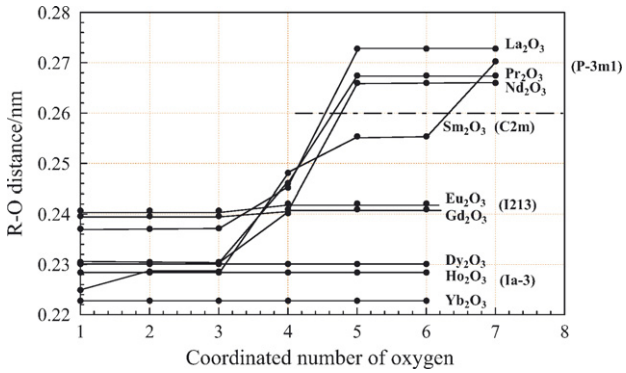

Fig. 13. Correlation between CN and distance between the rare earth ion and coordinated oxygens of the rare earth oxides.

and 6 is comparable to that for CN = 1–3 for R = Dy–Lu, a large difference is observed especially for R = La–Nd. The observed difference between light rare earth and heavy rare earth is related to the geometrical ball closed packing stacking model (difference in the radius ratio, $r(R^{3+})/r(O^{2-})$).

The lattice parameters of Li-free rare earth dioxycarbonates were estimated from this work for R = La, Pr, Nd, Sm, Eu and Gd. The estimated parameters are linearly increased with the radii of the R-ion. The lattice parameters for heavy rare earths are interpreted by the exploration method using the data for light rare earth dioxycarbonates. Furthermore, it is assumed that the relative position of the ion is not changed with the R species. By these assumptions, the distance between the R-ion and the coordinated oxygen for the rare earth dioxycarbonates could be interpreted, and the results are also indicated in Fig. 14. The comparison of the results for the R_2O_3 (Fig. 12) and $R_2O_2CO_3$ (Fig. 14) induced the result where the formation of $R_2O_2CO_3$ from R_2O_3 for R = Dy–Lu is achieved by prolonging the R–O distance for CN = 5 and 6. Roughly speaking, the formation of the corresponding oxycarbonate is achieved by the shortening of the R–O distance for CN = 5 for light rare earth metals such as R = La, Pr, Nd, and Sm. It seems that the formation of oxycarbonate from the oxide is easier for the light rare earth oxide than for the heavy rare earth oxides. The fact that the formation of oxycarbonate progresses for R = La–Gd but not for R = Dy–Lu

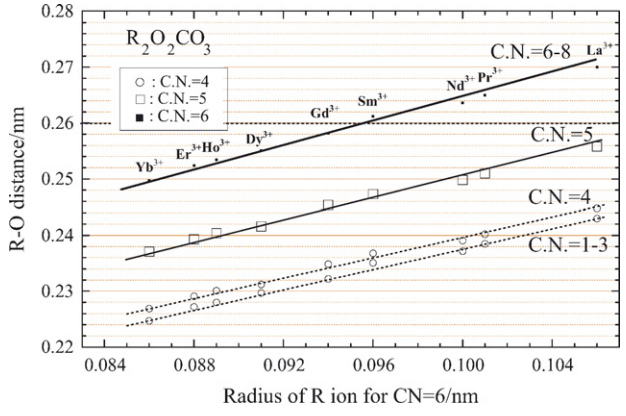

Fig. 14. Distance between the rare earth ion and coordinated oxygens of the Li-free rare earth oxycarbonate.

agrees with the CN stability of the rare earth oxides (Fig. 11). These results suggest that the driving force for the formation of the oxycarbonates is the difference in the stability between the sixfold- and eightfold-coordinations of oxygen. Based on these results, the high reactivity of the light rare earth oxides with Li_2CO_3 would be attributed to that the large R^{3+}–O^{2-} distance for CN = 5 and 6 with the increase in ionic $[R^{3+}]/[O^{2-}]$ ratio for the rare earth oxides and is very similar to that of the rare earth dioxymonocarbonates.

5. Conclusion

We investigated the reactivity of Li_2CO_3 and the rare earth oxides and the stability of the obtained products in syn-air and CO_2. In ambient CO_2, rare earth dioxymonocarbonate was formed by heating the mixture for R = La, Pr, Nd, Sm, Eu, and Gd to 500 °C and higher. Lithiation of their rare earth dioxymonocarbonates, i.e., $R_2O_{2+2x}(CO_3)_{1-x}Li_{2x}$, was confirmed for R = La, Pr, Nd, and Sm when the mixture was heated at 900 °C. The lithiation degree, x, was increased with an increase in the heat-treatment temperature in CO_2 and was lower than 0.3. The stability of the rare earth dioxymonocarbonates decreased with the atomic number of the rare earth. The reactivity and the stability are well related to the crystal structure of the rare earth oxide. For R = Ho–Yb, the carbonate could not be detected but the Li_2CO_3 phase became more stable due to the treatment in CO_2. The stability of Li_2CO_3 over its melting point may be attributed to the formation of nonstoichiometric rare earth carbonate compounds, $R_2O_3{\cdot}yCO_2$ and $Li_2O{\cdot}R_2O_3{\cdot}yCO_2$, on particles of the rare earth oxide.

References

1. Imanaka, N., Kawasato, T. and Adachi, G., A carbon dioxide gas sensor probe based on a lithium ionic conductor. *Chem. Lett.*, 1990, **1990**, 497–500.
2. Yao, S., Shimizu, Y., Miura, N. and Yamazoe, N., Solid electrolyte carbon dioxide sensor using binary carbonate electrode. *Chem. Lett.*, 1990, **1990**, 2033–2036.
3. Sadaoka, Y., Sakai, Y. and Manabe, T., CO_2 sensing characteristics of a solid-state electrochemical sensor based on a sodium ionic conductor. *J. Mater. Chem.*, 1992, **2**, 945–947.
4. Sadaoka, Y., Sakai, Y., Matsumoto, M. and Manabe, T., Solid-state electrochemical CO_2 gas sensors based on sodium ionic conductors. *J. Mater. Sci.*, 1993, **28**, 5783–5792.
5. Maruyama, T., Sakai, S. and Saito, Y., Potentiometric gas sensor for carbon dioxide using solid electrolytes. *Solid State Ionics*, 1987, **23**, 107–112.
6. Holzinger, M., Maier, J. and Sitte, W., Fast CO_2-selective potentiometric sensor with open reference electrode. *Solid State Ionics*, 1996, **86–88**, 1055–1062.
7. Kida, T., Shimanoe, Miura, N. and Yamazoe, N., Stability of NASICON-based CO_2 sensor under humid conditions at low temperature. *Sens. Actuators B*, 2001, **75**, 179–187.
8. Uemura, H. and Matsui, M., Solid electrolyte CO_2 sensor fabricated with $LiCO_3$–$La_{9.33}Si_6O_{26}$ as sensing electrode. *J. Ceram. Soc. Jpn.*, 2002, **110**, 51–54 [in Japanese].
9. Kale, G. M., Davison, A. J. and Fray, D. J., Investigation into an improved design of CO_2 sensor. *Solid State Ionics*, 1996, **86–88**, 1107–1110.
10. Chu, W. F., Fischer, D., Erdmann, H., Ilgestei, M., Köppen, H. and Leonard, V., Thin and thick film electrochemical CO_2 sensors. *Solid State Ionics*, 1992, **53–56**, 80–84.

11. Alonso-Porta, M. and Kumar, R. V., Use of NASICON/Na_2CO_3 system for measuring CO_2. *Sens. Actuators B*, 2000, **71**, 173–178.
12. Imanaka, N., Kamikawa, M. and Adachi, G., A carbon dioxide gas sensor by combination of multivalent cation and anion conductors with a water-insoluble oxycarbonate-based auxiliary electrode. *Anal. Chem.*, 2002, **74**, 4800–4804.
13. Tamura, S., Hasegawa, I., Imanaka, N., Maekawa, T., Tsumiishi, T., Suzuki, K. *et al.*, Carbon dioxide gas sensor based on trivalent cation and divalent oxide anion conducting solids with rare earth oxycarbonate based auxiliary electrode. *Sens. Actuators B*, 2005, **108**, 359–363.
14. Attfield, J. P. and Ferey, G., Structure determinations of $La_2O_2CO_3$-II and the unusual disordered phase $La_2O_{2.52}(CO_3)_{0.74}Li_{0.52}$ using powder diffraction. *J. Solid State Chem.*, 1989, **82**, 132–138.
15. Aono, H., Itagaki, Y. and Sadaoka, Y., $Na_3Zr_2Si_2PO_{12}$-based CO_2 gas sensor with heat-treated mixture of Li_2CO_3 and Nd_2O_3 as an auxiliary electrode, *Sens. Actuators B*, in press.
16. Yamauchi, M., Itagaki, Y., Aono, H. and Sadaoka, Y., Preparation and characterization of a novel lithium-inserted light rare earth dioxycarbonate (La and Nd). *J. Ceram. Soc. Jpn.*, 2007, **114**(6), 363–369.
17. Preiss, J. and Dussik, A., Bildungsverhältnisse und hydrolyse der ceriterdkarbonate. *Z. Anorg. Allg. Chem.*, 1923, **131**, 275–286.
18. Wakita, H., The synthesis of hydrated rare earth carbonate single crystals in gels. *Bull. Chem. Soc. Jpn.*, 1978, **56**, 2879–2881.
19. Turcotte, R. P., Sawyer, J. O. and Eyring, L., On the rare earth dioxymonocarbonates and their decomposition. *Inorg. Chem.*, 1969, **8**, 238–246.
20. Caro, P., Achard, J. C. and de Pous, O., Les elements des terres rares. Colloques Intern. du CNRS, No. 180, *Vol. 1*, 1970, p. 287.
21. Kalz, H.-J. and Seidel, H., Lithium-lanthanoid-carbonate und lithium-lanthanoid-oxycarbonate. *Z. Anorg. Allg. Chem.*, 1980, **465**, 92–108.
22. Gschneidner Jr., K. A. and Eryring, L. ed., *Handbook on the Physics and Chemistry of Rare Earths*, *Vol. 3*. North-Holland Publishing Co., Amsterdam, 1979, p. 564.